

Resonance peak shift in the photo-current of ultrahigh-mobility two-dimensional electron systems.

Jesús Iñarra^{1,2}

¹*Escuela Politécnica Superior, Universidad Carlos III, Leganes, Madrid, 28911, Spain*

²*Unidad Asociada al Instituto de Ciencia de Materiales, CSIC, Cantoblanco, Madrid, 28049, Spain.*

We report on a theoretical study on the rise of strong peaks at the harmonics of the cyclotron resonance in the irradiated magnetoresistance in ultraclean two-dimensional electron systems. The motivation is the experimental observation of a totally unexpected strong resistance peak showing up at the second harmonic. We extend the radiation-driven electron orbit model (previously developed to study photocurrent oscillations and zero resistance states) to a ultraclean scenario that implies longer scattering time and longer mean free path. Thus, when the mean free path is equivalent, in terms of energy, to twice the cyclotron energy ($2\hbar\omega_c$), the electron behaves as under an effective magnetic field twice the one really applied. Then, at high radiation power and/or low temperature, a resistance spike can be observed *at the second harmonic*. For even cleaner samples the energy distance could increase to three or four times the cyclotron energy giving rise to resistance peaks at higher harmonics (third, fourth, etc.), i.e., a resonance peak shift to lower magnetic fields as the quality of the sample increases. Thus, by selecting the sample mobility one automatically would select the radiation resonance response without altering the radiation frequency.

PACS numbers:

Radiation-induced magnetoresistance (R_{xx}) oscillations (MIRO)^{1,2}, show up in high mobility two-dimensional electron systems (2DES) when they are irradiated with microwaves (MW) at low temperatures ($T \sim 1K$) and under low magnetic fields (B) perpendicular to the 2DES. At high enough radiation power (P) oscillations maxima and minima increase but the latter evolve into zero resistance states (ZRS)^{1,2}. Both effects were totally unexpected when they were first obtained revealing some type of new radiation-matter interaction assisting electron magnetotransport^{3,4}. Their discovery was considered very important, specially in the case of zero resistance states, because they were obtained without quantization in the Hall resistance. Despite the fact that over the last years quite a few important experimental⁵⁻²¹ and theoretical efforts²²⁻³⁶ have been made on MIRO and ZRS, their physical origin still remains unclear and controversial.

Resonance phenomena can be found widely in nature and occur with all type of oscillations from sound to electromagnetic radiation. They are extremely interesting in physics, from theoretical to applications perspectives, because they give rise to an intense energy transfer between an exciting source and a driven systems. But it turns out definitively more intriguing and puzzling when the resonance takes place off the natural oscillation frequency. This applies to one of the most challenging experimental findings^{37,38} regarding MIRO and as unexpected as ZRS. It consists of a prominent resistance peak that shows up at the second harmonic of the cyclotron frequency, $\omega \simeq 2 \times \omega_c$, (ω is the radiation frequency and ω_c the cyclotron frequency) in irradiated R_{xx} ^{37,38} of ultrahigh mobility 2DES. This extremely high mobility ($\mu \geq 3 \times 10^7 \text{ cm}^2/\text{Vs}$) along with a low T and high P play an essential role in the appearance of this striking result. The amplitude of such a spike is very large

regarding the usual MIRO, suggesting a resonance effect but off the expected position: $\omega \simeq \omega_c$. To date, there have been presented very few theoretical models on this topic^{39,40}.

In this article, we present a theoretical analysis on this resonance peak shift based on the radiation-driven electron orbit model^{22,23} but adapted to a scenario of ultra high quality samples (reduced electron scattering). In the extension of the model we start considering that this kind of samples have increasingly longer both mean free path and scattering time. Thus, the scattered electron that jumps between Landau orbits (Landau states) can reach much further, in distance and energy, final Landau orbits (due to the DC electric field applied in the x direction, see Fig. 1). For instance, orbits located at twice the cyclotron energy ($2\hbar\omega_c$). For this specific case the electron would behave, from the scattering standpoint, as under an *effective* magnetic field of double intensity than the one really applied. Then, the spike will rise, at low enough T and high enough P , at the second harmonic. For even higher mobilities we would still have longer mean free paths and then, we can predict the subsequent rise of R_{xx} spikes at higher harmonics: $3\omega_c = \omega$, $4\omega_c = \omega$, $5\omega_c = \omega$, etc., i.e., at lower and lower B . Therefore and as a main result, we conclude that by controlling the mobility of 2DES we can shift the resonance response without altering the radiation frequency. This result could turn out very interesting for device engineering and applications. For instance, irradiating a ultraclean 2D sample with Terahertz radiation we would obtain a resonance response in a B region corresponding to MW or even lower frequencies.

Another important result from our theoretical model is that both MIRO and R_{xx} spike would share the same physical origin. Thus, they would stem from the interplay of the radiation-driven swinging motion of the irra-

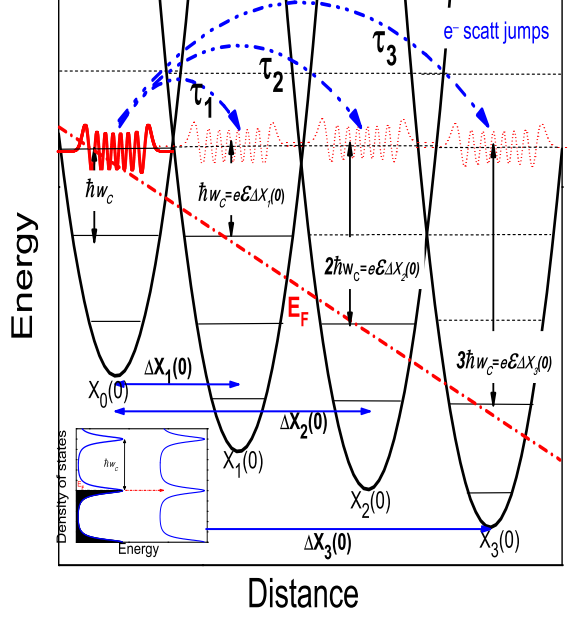


FIG. 1: Schematic diagram describing elastic scattering between tilted Landau orbits (Landau states) according to $n\hbar w_c = e\xi\Delta X_n(0)$. ξ is the DC driving electric field and $X_n(0)$ are the positions of the corresponding Landau orbits. The maximum contribution to the current is obtained when the Landau levels involved in the scattering jumps are aligned, (see inset).

diated Landau orbits and the scattering of electrons with charged impurities. Thus, the large R_{xx} spike would correspond to a resonance effect between the frequency of the Landau orbit harmonic motion and w_c . Obviously the former turns out to be the same as radiation frequency.

The *radiation-driven electron orbits model*, was devised by the authors to address two physical effects triggered by radiation: MIRO and ZRS in high mobility 2DES. According to this model, under radiation the Landau orbits, spatially and harmonically oscillate with the radiation frequency. As a result, the scattering process of electrons with charged impurities turns out to be dramatically altered. This is reflected in magnetotransport and in turn in R_{xx} giving rise to the well-known MIRO and ZRS^{22,23,41–43}. Following the model, we use a semiclassical Boltzmann theory to calculate the longitudinal conductivity σ_{xx} ^{44–46}:

$$\sigma_{xx} = 2e^2 \int_0^\infty dE \rho_i(E) (\Delta X)^2 W_I \left(-\frac{df(E)}{dE} \right) \quad (1)$$

being E the energy and $\rho_i(E)$ the density of initial Landau states. The expression for ΔX is likewise obtained from the model^{47,48}:

$$\Delta X = \Delta X_1(0) - A(w_c) \sin(w\tau_1) \quad (2)$$

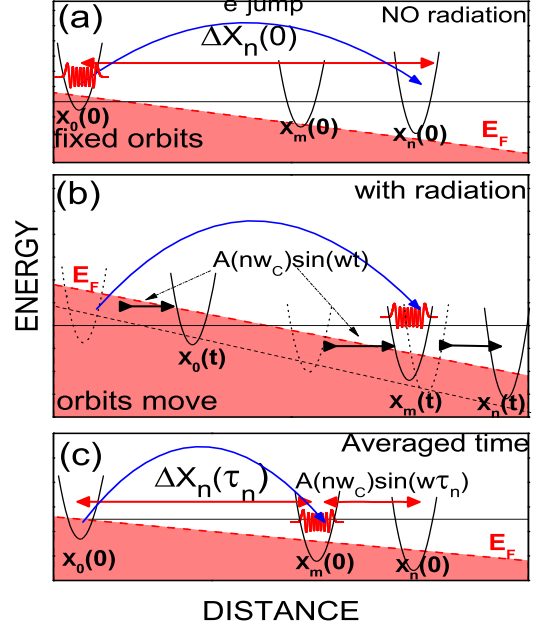


FIG. 2: Schematic diagrams for the emergence of a valley in MIRO in an extended scenario (distant Landau orbits). (a) Elastic scattering (charged impurities) between Landau orbits without radiation. (b) Elastic scattering with radiation where all Landau orbits oscillate at radiation frequency. The $X_n(0)$ position is occupied now by a driven-Landau orbit, $X_m(0)$, where the scattered electron lands in a time $t = \tau_n$. (c) With radiation but in the steady state after time average. The final averaged distance is smaller than in the dark giving rise to a MIRO valley. Similar reasoning can be applied for a MIRO peak.

where $\Delta X_1(0)$ is the distance between the guiding centers of the final and initial Landau orbits in the dark and $\tau_1 = 2\pi/w_c$ is the *flight time*: the time it takes the scattered electron between Landau orbits. It was previously proposed, in a semiclassical approach^{47,49}, that during the scattering jump electrons in their orbits would complete, on average, an integer number of cyclotron orbits, which implies that $\tau_n = n \times T_c = n \times \frac{2\pi}{w_c}$, T_c being the cyclotron time. Therefore, the carrier involved in the scattering ends up in the same relative position inside the final orbit as the one it started from in the initial one. The reason for this is that the dynamics of the orbits (Landau states) is governed on average by the position of the centre of the orbit irrespective of the carrier position inside the orbit when the scattering takes place. Then, on average, both the initial and final semiclassical positions are identical in their respective orbits. In the radiation-driven electron orbit model^{47,48} $n = 1$ and $\tau_1 = T_c$ corresponding to one cyclotron orbit during the jump. $A(w_c)$ is the amplitude of the spatial oscil-

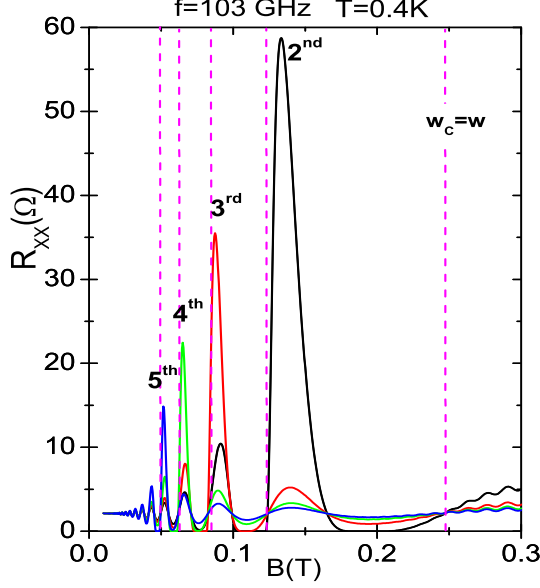


FIG. 3: Calculated magnetoresistance vs B under radiation of 103GHz and $T = 0.4\text{K}$ for four resonance regimes: $2w_c = w$, $3w_c = w$, $4w_c = w$ and $5w_c = w$. Vertical dashed lines mark the harmonic positions. Spikes rise up from the second to fifth harmonic. The photo-excited oscillations positions remain constant showing the $1/4$ cycle phase shift independently of the resonance peak displacement.

lations of the driven orbits in the x direction: $A(w_c) = \frac{eE_0 \sin wt}{m^* \sqrt{w^2(w_c - w)^2 + \gamma^4}}$, E_0 being the radiation electric field and γ is a damping parameter related to the interaction of the electrons in the driven Landau orbits with the lattice ions. W_I is the scattering rate of electrons with charged impurities that according to the Fermi's golden rule: $W_I = \frac{2\pi}{\hbar} |\langle \phi_f | V_s | \phi_i \rangle|^2 \delta(E_i - E_f)$, where ϕ_i and ϕ_f are the wave functions corresponding to the initial and final Landau states respectively and V_s is the scattering potential for charged impurities⁴⁵. The expressions of the initial and final energies are: $E_i = \hbar w_c(i + 1/2)$ and $E_f = \hbar w_c(f + 1/2) - \Delta_{DC}$, where i and f are integers and $\Delta_{DC} = e\xi \Delta X(0)$, ξ is the DC driving electric field in the x direction and responsible of the current along that direction (see Fig. 1). To obtain R_{xx} we use the common tensorial relation $R_{xx} = \frac{\sigma_{xx}}{\sigma_{xx}^2 + \sigma_{xy}^2} \simeq \frac{\sigma_{xx}}{\sigma_{xy}^2}$, where $\sigma_{xy} \simeq \frac{n_i e}{B}$, n_i being the electrons density, e the electron charge and $\sigma_{xx} \ll \sigma_{xy}$.

According to W_I the largest contributions to the conductivity in the presence of the field ξ occurs when $E_i = E_f \Rightarrow e\xi \Delta X_n(0) \simeq n \times \hbar w_c$, implying that the Landau level indexes, f and i are related by $f = i + n$, n being a positive integer. Or in other words, when the Landau levels are aligned (see inset in Fig.1). The $n = 1$ scenario labelled with τ_1 in Fig.1, implies that $e\xi \Delta X_1(0) = \hbar w_c$ and it would correspond to ordinary MIRO. In a general

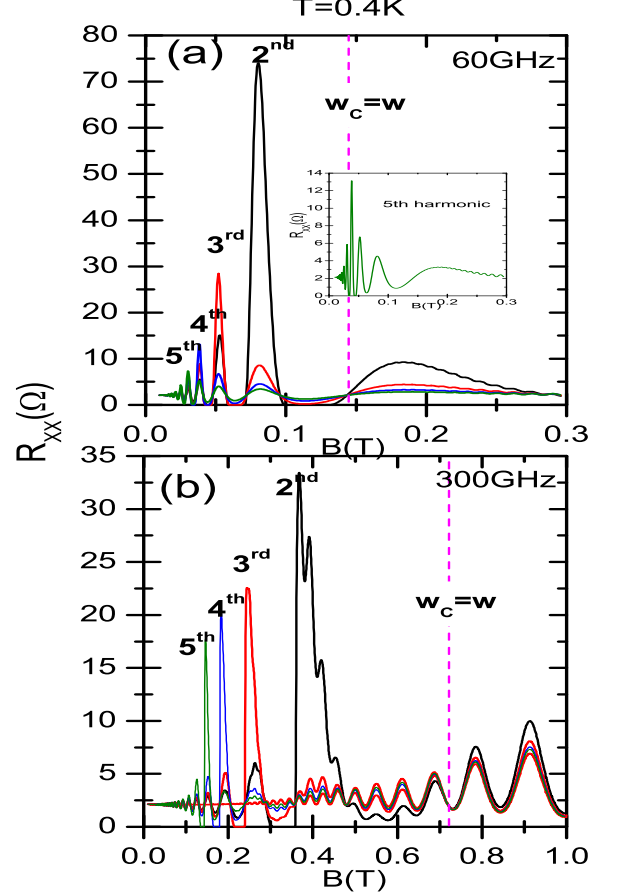


FIG. 4: Same as in Fig.3. We exhibit the same four off-resonance spikes for 60GHz in panel (a) and for 300GHz in panel (b). The vertical dashed line for both panels corresponds to the main resonance frequency. The inset in panel (a) is a zoom-in of the fifth harmonic.

extension of the model we can include other scattering processes that are, likewise, likely to happen according to W_I (their Landau levels are aligned too). These processes are labelled in Fig.1, with τ_2 and τ_3 (flight times of these processes) and correspond to energy differences (in reference to the Fermi energy) of $e\xi \Delta X_2(0) = 2\hbar w_c$ and $e\xi \Delta X_3(0) = 3\hbar w_c$ respectively (see Fig.1). Yet, the long distance between the Landau orbits involved in the scattering (longer than the mean free path in ordinary samples) prevent them from happening; the corresponding probability is very small. Accordingly, and in light of the uncertainty principle⁵⁰, the minimum values of those flight times can be obtained: $\tau_2 = 2\pi/2w_c$ and $\tau_3 = 2\pi/3w_c$ respectively. Thus, we obtain increasingly shorter flight times in increasingly longer scattering times. And the flight times get smaller not in a continu-

ous way but by integer values of w_c in the denominator.

Interestingly enough and according to the above, the process labelled with τ_2 would be mainly described by scattering quantities such as the distance between Landau orbits, $\Delta X_2(0)$ and the corresponding flight time, being both given by:

$$e\xi\Delta X_2(0) = \hbar w_c^* \quad (3)$$

$$\tau_2 = \frac{2\pi}{w_c^*} \quad (4)$$

where $\hbar w_c^* = \hbar \frac{eB^*}{m^*} = \hbar \frac{e(2B)}{m^*} = 2\hbar w_c$. Then, from the scattering point of view, we would obtain the same re-

sults as if the electron were under an effective twice as high magnetic field (B^*) than the one really applied (B). Similar approach can be applied to the τ_3 and further scenarios. Thus, for τ_3 we would have and effective magnetic field $B^{**} = 3B$ and $w_c^{**} = 3w_c$. Therefore in our model the increasing quality of the sample makes vary the main scattering quantities in steps, i.e., in integer values of w_c . The above discussion is essential for the model and would be at the heart of the experimental results as we explain below. Now, applying the theory of radiation driven electron orbit model⁴⁸ to these new scenarios, (from τ_1 to τ_2 and τ_3 etc.), we obtain a general expression for ΔX ,

$$\Delta X = [\Delta X_1(0) - A(w_c) \sin(w\tau_1)] + [\Delta X_2(0) - A(w_c^*) \sin(w\tau_2)] + [\Delta X_3(0) - A(w_c^{**}) \sin(w\tau_3)] + \dots \quad (5)$$

where $A(w_c^*) = \frac{eE_0 \sin wt}{m^* \sqrt{w^2(w_c^* - w)^2 + \gamma^4}}$ and $A(w_c^{**}) = \frac{eE_0 \sin wt}{m^* \sqrt{w^2(w_c^{**} - w)^2 + \gamma^4}}$. And accordingly, we could obtain the resonance peak in different B -positions depending on what is the predominant term over the rest. In the general expression above, we have extended the basic idea of our model that when the radiation is on, the Landau orbits oscillate (driven by radiation) altering the electron scattering. And for different flight times (depending of the scenario) $\tau_n = 2\pi/nw_c$, the scattered electron will be *landing* in a different final Landau orbit and different in turn from the dark giving rise to a distance shift in the scattering jump. After averaging out, the shift is given by $A(nw_c) \sin(w\tau_n)$ (see Fig. 2). This shift can be positive or negative (or zero) and is finally reflected in σ_{xx} and R_{xx} in the form of peaks and valley respectively, i.e., photo-excited R_{xx} oscillations or MIRO.

As we said above, in an ordinary MIRO experiment only the expression of the first bracket in the right part of the latter equation, (the $[\Delta X_1(0) - A(w_c) \sin(w\tau_1)]$ term), would significantly contribute to ΔX . In this regime the shorter mean free path prevent from reaching further Landau orbits making negligible the contributions of the other terms. Nevertheless, when it comes to ultrahigh mobility samples we will have longer mean free paths and scattering times, and much further final Landau orbits can be accessible via scattering. Thus, by increasing mobility we would end up having first the $[\Delta X_2(0) - A(2w_c) \sin(w\tau_2)]$ term as predominant where the resonance peak would rise at the second harmonic. In a next step increasing further mobility even more distant Landau orbits would be accessible and thus, we would obtain the third term, $([\Delta X_3(0) - A(3w_c) \sin(w\tau_3)])$, as predominant and the resonance at the third harmonic, etc. For instance, what it is obtained in the off-resonance experiments^{37,38} would be based on the second term and the expression of the average advanced distance would

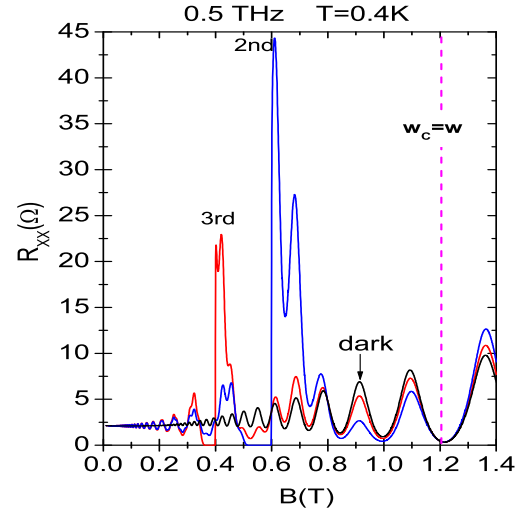


FIG. 5: Same as in Fig.3., for a frequency of $0.5 THz$. We exhibit two off-resonance spikes for the second and third harmonic positions. The vertical dashed line corresponds to the main resonance frequency.

be: $\Delta X \simeq [\Delta X_2(0) - A(2w_c) \sin(w\tau_2)]$. But still the flight time τ_2 needs to be adapted to a ultra-clean scenario, i.e., it has to be increased as the scattering time increases too. As we said above in our model, this increment has to be made in multiples of T_c corresponding to the effective magnetic field. This implies that now the new $\tau_2 = 2 \times 2\pi/2w_c$. Substituting in ΔX , we finally obtain: $\Delta X \simeq [\Delta X_2(0) - A(2w_c) \sin(2\pi \frac{w}{w_c})]$. The latter is a remarkable result because it can be generalized to higher order terms where, as the magnetoresistance resonance peak shifts to lower B , the photo-excited os-

cillations (MIRO) would remain at the same B -position. This is in agreement with experiments^{37,38}.

In Fig. 3 we exhibit the calculated magnetoresistance vs B under radiation of 103GHz and $T = 0.4\text{K}$. We present four curves each one corresponding to a different resonance regime: $2w_c = w$, $3w_c = w$, $4w_c = w$ and $5w_c = w$. Spikes are obtained from the second to fifth harmonic. The harmonic positions are given by the dashed vertical lines (including the main resonance). And as explained above, the oscillations positions remain constant showing the $1/4$ phase shift independently of the resonance peak displacement that moves to lower B for each harmonic. In Fig.4 we present similar results to Fig.3 but for two distant frequencies of the microwave band to prove that the off-resonance spikes are a generic feature of MIRO. However they can only be observed clearly with ultraclean 2DES, cleaner than the ordinary conditions to observe MIRO and ZRS. We exhibit the four off-resonance spikes for 60GHz in panel (a) and for 300GHz in panel (b). The vertical dashed line for both panels corresponds to the main resonance frequency. In Fig. 5 we exhibit calculated results corresponding to the terahertz band for a radiation frequency of 0.5THz . Thus, we present the same as in Fig.3 but for only two irradiated curves corresponding to the $2w_c = w$ and $3w_c = w$ resonance regimes. Thus, on the one hand,

we want to demonstrate that this effect can show up at higher frequencies than the microwave band proving that it can be considered as a universal effect. And, on the other hand, from the application standpoint it might be interesting to stress that for a terahertz frequency we can obtain the resonance response clearly inside the microwave range just by increasing the mobility of the sample.

In summary, we have presented a theoretical approach on the off-resonance spikes generation in irradiated magnetoresistance in ultraclean 2DES. We have explained the experiments where the spike at the second harmonic is obtained and predict the appearance of subsequent spikes at higher harmonics for higher mobilities. We have explained this striking effect from the perspective of the radiation-driven electron orbits model based on the idea that this kind of samples have a longer mean free path. Thus, when, in terms of energy, this distance is twice the cyclotron energy, the electron behaves as under an effective B double than the one really applied. Then a resistance spike *at the second harmonic* can be observed.

This work is supported by the MINECO (Spain) under grant MAT2017-86717-P and ITN Grant 234970 (EU). GRUPO DE MATEMATICAS APLICADAS A LA MATERIA CONDENSADA, (UC3M), Unidad Asociada al CSIC.

-
- ¹ R. G. Mani, J. H. Smet, K. von Klitzing, V. Narayana-murti, W. B. Johnson, and V. Umansky, Nature(London) **420**, 646 (2002)
 - ² M. A. Zudov, R. R. Du, L. N. Pfeiffer, and K. W. West, Phys.Rev. Lett. **90**, 046807 (2003)
 - ³ J. Iñarrea and G. Platero Physica Status Solidi (a) **203**, 1148 (2006).
 - ⁴ J. Iñarrea, R. Aguado, G. Platero, Europhys Lett. **40**, 417, (1997)
 - ⁵ R. G. Mani, J. H. Smet, K. von Klitzing, V. Narayana-murti, W. B. Johnson, and V. Umansky, Phys. Rev. Lett. **92**, 146801 (2004).
 - ⁶ R. G. Mani, J. H. Smet, K. von Klitzing, V. Narayana-murti, W. B. Johnson, and V. Umansky, Phys. Rev. **B69**, 193304 (2004).
 - ⁷ R. L. Willett, L. N. Pfeiffer, and K. W. West, Phys. Rev. Lett. **93**, 026604 (2004).
 - ⁸ R. G. Mani, Physica E (Amsterdam) **22**, 1 (2004);
 - ⁹ J. H. Smet, B. Gorshunov, C. Jiang, L. Pfeiffer, K. West, V. Umansky, M. Dressel, R. Meisels, F. Kuchar, and K. von Klitzing, Phys. Rev. Lett. **95**, 118604 (2005).
 - ¹⁰ Z. Q. Yuan, C.L. Yang, R.R. Du, L.N. Pfeiffer and K.W. West, Phys. Rev. **B74**, 075313 (2006).
 - ¹¹ R. G. Mani, W.B. Johnson, V. Umansky, V. Narayanamurti and K. Ploog, Phys. Rev. **B79**, 205320 (2009).
 - ¹² S. Wiedmann, G.M. Gusev, O.E. Raichev, A.K. Bakarov, and J.C. Portal, Phys. Rev. Lett., **105**, 026804, (2010)
 - ¹³ S. Wiedmann, G.M. Gusev, O.E. Raichev, A.K. Bakarov, and J.C. Portal, Phys. Rev. **B**, **81**, 085311, (2010)
 - ¹⁴ D. Konstantinov and K. Kono, Phys. Rev. Lett. **103**, 266808 (2009)
 - ¹⁵ S. I. Dorozhkin, L. Pfeiffer, K. West, K. von Klitzing, J.H. Smet, JH, NATURE PHYSICS, **7**, 336-341, (2011)
 - ¹⁶ R. G. Mani, C. Gerl, S. Schmult, W. Wegscheider and V. Umansky, Phys. Rev. **B81**, 125320, (2010)
 - ¹⁷ R.G. Mani, A.N. Ramanayaka and W. Wegscheider, Phys. Rev. **B**, **84**, 085308, (2011)
 - ¹⁸ Jesus Inarrea, R.G. Mani and W. Wegscheider, Phys. Rev. **B**, **82** 205321 (2010)
 - ¹⁹ R. G. Mani, Int. J. Mod. Phys. **B**, **18**, 3473, (2004); Physica **E**, **25**, 189 (2004)
 - ²⁰ Tianyu Ye, Han-Chun Liu, W. Wegscheider and R.G. Mani, Phys. Rev. **B**, **89**, 155307, (2014)
 - ²¹ TY Ye, HC Liu, Z Wang, W Wegscheider, RG Mani, Scientific Reports, **5**, 14880, (2015)
 - ²² J. Iñarrea and G. Platero, Phys. Rev. Lett. **94** 016806, (2005)
 - ²³ J. Iñarrea and G. Platero, Phys. Rev. **B** **72** 193414 (2005)
 - ²⁴ Jesus Iñarrea, Appl. Phys. Lett. **100**, 242103 (2012).
 - ²⁵ J. Inarrea and G. Platero. Phys. Rev. **B**, **84**, 075313, (2011).
 - ²⁶ Jesus Iñarrea, Appl. Phys. Lett. **99**, 232115 (2011).
 - ²⁷ A.C. Durst, S. Sachdev, N. Read, S.M. Girvin, Phys. Rev. Lett. **91** 086803 (2003)
 - ²⁸ X.L. Lei, S.Y. Liu, Phys. Rev. Lett. **91**, 226805 (2003)
 - ²⁹ Ryzhii et al, Sov. Phys. Semicond. **20**, 1299, (1986)
 - ³⁰ P.H. Rivera and P.A. Schulz, Phys. Rev. **B** **70** 075314 (2004)
 - ³¹ J. Iñarrea and G. Platero, Phys. Rev. **B**, **78**, 193310, (2008)
 - ³² J. Iñarrea, Appl. Phys Lett. **92**, 192113, (2008)
 - ³³ Jesus Inarrea and Gloria Platero, Appl. Phys. Lett. **95**,

- 162106, (2009);
- ³⁴ J. Inarrea, Appl. Phys Lett. **90**, 262101,(2007)
- ³⁵ J. Inarrea , C. Lopez-Monis , A.H. MacDonald and G. Platero , Appl. Phys. Lett., **91**, 252112, (2007)
- ³⁶ Jesus Inarrea, J. Appl. Phys., bf 113 183717 (2013)
- ³⁷ Yanhua Dai, R.R. Du, L.N. Pfeiffer and K.W. West, Phys. Rev. Lett., **105**, 246802, (2010).
- ³⁸ A.T. Hatke, M.A. Zudov, L.N. Pfeiffer and K.W. West, Phys. Rev. B **83**, 121301(R), (2011).
- ³⁹ J. Inarrea, Physica Status Solidi-Rapid Research Letters, **6**, 394, (2012).
- ⁴⁰ VA Volkov, AA Zabolotnykh, Phys. Rev. B, **89**, 121410 (2014).
- ⁴¹ J. Inarrea and G. Platero, Appl. Physl Lett. **89**, 172114, (2006)
- ⁴² E.H. Kerner, Can. J. Phys. **36**, 371 (1958).
- ⁴³ K. Park, Phys. Rev. B **69** 201301(R) (2004).
- ⁴⁴ B.K. Ridley. *Quantum Processes in Semiconductors*, 4th ed. Oxford University Press, (1993).
- ⁴⁵ T. Ando, A. Fowler and F. Stern, Rev. Mod. Phys.**54**,(1982)
- ⁴⁶ Noboru Miura, *Physics of Semiconductors in High Magnetic Fields.*, Oxford University Press, (2008).
- ⁴⁷ Jesus Inarrea and Gloria Platero. Journal of Physics:Condens. Matter, **27** 415801 (2015)
- ⁴⁸ Jesus Inarrea, Sci. Rep. **7**, 13573, (2017).
- ⁴⁹ P E Brito and H N Nazareno. Eur. J. Phys. **28**, 9, (2007)
- ⁵⁰ Claude Cohen-Tannoudji, Bernard Diu and Franck Laloe, *Qauntum Mechanics*, John Wiley and sons, New York, (1977).